Experimental Study Exploring the Interaction of Structural and Leakage Dynamics

Sam Fox, Ph.D.[1]; Richard Collins, Ph.D.[2]; and Joby Boxall[3]

Abstract: Strategies for managing leakage from water distribution systems require the ability to effectively evaluate such real losses through the understanding of the behavior of individual leaks, including their response to changes in pressure regime due to demand or management strategies. This paper presents the results from an innovative experimental investigation aimed at understanding the response of longitudinal slits in pressurized viscoelastic pipes, specifically considering the interaction between the structural and leakage dynamics. For the first time, leakage flow rate, pressure, leak area, and material strain were recorded simultaneously, providing new knowledge of the complex interaction of these factors. The paper shows that strain and area are directly related, hence it is possible to employ strain as a predictor of leak area, calculated using a calibrated viscoelastic model. Using such an approach, the leakage flow rates under a range of quasi-static pressures were accurately predicted and validated. Overall the paper demonstrates that the orifice equation, with a constant coefficient of discharge, is suitable for accurately estimating dynamic leakage flow rates from longitudinal slits, provided that the leak area is suitably incorporated. **DOI: 10.1061/(ASCE)HY.1943-7900.0001237.**

Author keywords: Leakage; Structure; Viscoelasticity; Dynamics; Discharge coefficient.

Introduction

Leakage remains a key sustainability issue faced by water utilities around the world. Estimates for the level of leakage in the United Kingdom alone highlight the significance of the problem, with Ofwat (2013) published figures estimating that 23.6% of the total distributed water was lost through bursts and background leakage between 2012 and 2013. This figure has reduced marginally during the last decade under the current economic levels of leakage (ELL) directive (Strategic Management Consultants 2012). Leakage management strategies aimed at addressing this issue range from the development of leak detection technologies to advanced pressure management schemes. Likewise, the selection of pipe material is also targeted at improving the durability and cost-effectiveness of distribution systems by minimizing the occurrence of pipe failures. Polyethylene pipes in particular offer cost benefits due to their inherent durability and flexibility resulting in ease of installation and tolerance to potential ground movement (GPS-UK 2014). Plastic pipes are often perceived as a leak-free option; however, this is not evident in practice. Understanding the leakage behavior of leaks that occur in plastic pipes is crucial in planning and implementing effective active leakage control strategies.

Background

Leakage modeling plays a major part in the process of leakage management in water distribution systems. This includes the quantification and/or estimation of leakage levels in operational systems (Thornton and Lambert 2005; Cheung et al. 2010), application of leakage detection methodologies (Pudar and Liggett 1992; Vitkovsky et al. 2000; Koppel et al. 2009), and the development of effective pressure management schemes (Awad et al. 2008; Nazif et al. 2009). Such tools and techniques use leakage flow rate estimation based on Eq. (1), known as the orifice equation

$$Q = A_L C_d \sqrt{2gH} = ch^{\lambda} \tag{1}$$

The effectiveness of this equation has been reviewed by several authors who explore the variability of the relationship between pressure and leakage using a generalized form of the equation, also given in Eq. (1) (May 1994; Thornton and Lambert 2005; Clayton and van Zyl 2007).

The power term, λ, is theoretically constant equal to 0.5. However, field data and analyses at the district metered area (DMA) level (DMAs are manageable divisions of a larger distribution networks), as summarized by Farley and Trow (2003), found that the leakage exponents in Brazil, Japan, and the United Kingdom lay in the range 0.52–2.79. In addition, experimental investigations isolating individual leaks have shown that the theoretical value ($\lambda = 0.5$) is not appropriate or accurate in all cases. Greyvenstein and van Zyl (2006) conducted a series of tests on failed pipe sections from real systems and determined leakage exponent values ranging from 0.40 to 2.30. Leakage exponent values greater than 1.0 were noted predominantly for longitudinal cracks and corrosion clusters emphasizing the sensitivity of these particular leak types to changes in pressure. Similarly, Ávila Rangel and Gonzalez Barreto (2006) evaluated leakage exponents between 1.40 and 2.01 for manufactured longitudinal slits in PVC pipe. For the purpose of this paper, cracks are defined as naturally occurring pipe failures, while slits are artificially manufactured openings. The conclusion drawn from these studies was that leaks are more sensitive to pressure than is described by the simple orifice equation but that the additional pressure-dependent behavior can be modeled by the definition of a single-leakage exponent once the leak-specific behavior is known. This approach reflects the fixed and variable

[1]Dept. of Civil and Structural Engineering, Pennine Water Group, Univ. of Sheffield, Mappin St., Sheffield S1 3JD, U.K. (corresponding author). E-mail: sam.fox0509@gmail.com

[2]Dept. of Civil and Structural Engineering, Pennine Water Group, Univ. of Sheffield, Mappin St., Sheffield S1 3JD, U.K.

[3]Professor, Dept. of Civil and Structural Engineering, Pennine Water Group, Univ. of Sheffield, Mappin St., Sheffield S1 3JD, U.K.

Note. This manuscript was submitted on May 29, 2015; approved on July 1, 2016; published online on September 22, 2016. Discussion period open until February 22, 2017; separate discussions must be submitted for individual papers. This paper is part of the ***Journal of Hydraulic Engineering***, © ASCE, ISSN 0733-9429.

area discharge (FAVAD) model proposed by May (1994), with the observed sensitivity surmised to be predominantly influenced by the pressure dependence of leak opening areas (Clayton and van Zyl 2007). Ferrante et al. (2014) consider the consequence of quantifying the behavior of single or multiple leaks (global leaks), numerically confirming that the mean global leakage exponent is typically higher than the equivalent single-leakage exponent because it accounts for all the quantities affecting the distributed leakage. Application of the leakage exponent evaluated from physical observations of single leaks may, therefore, not be appropriate in all cases due to spatial and temporal variability affects.

An understanding of the effect of the dynamic nature of the opening area on leak hydraulics, specifically the definition of a coefficient of discharge, is a relatively unexplored topic within the literature. The effective leak area ($A_E = C_d A_L$), which captures the coupled definition of both the leak area and discharge coefficient, is often used. Theoretical and experimental investigations using this approach, for different failures, highlighted the pressure dependence of the effective leak area most notably for longitudinal cracks (Al-Khomairi 2005; Ferrante et al. 2011). However, this methodology does not facilitate assessment of the fundamental interdependence of the leak area and the coefficient of discharge. In other words, is the theoretical coefficient of discharge dependent on pressure and the dynamic leak area? Definition of the synchronous pressure, leak area, and subsequent leakage flow rate is necessary to evaluate the associated coefficient of discharge and fully validate the effectiveness of using the orifice equation when integrating the pressure-dependent leak area.

Commonly used pipe materials found in water distribution systems include steel, concrete, and ductile iron, which behave as linear-elastic materials. However, polymeric materials such as medium-density polyethylene (MDPE) are viscoelastic in nature. The use of such polymeric materials drives a need to understand the phenomena of viscoelasticity, which manifests as pressure, time, and temperature-dependent behavior. A relatively common failure type in viscoelastic pipes such as polyethylene are longitudinal cracks (axial direction), a brittle failure mode, which form in the direction of extrusion (Grann-Meyer 2005; O'Connor 2011). Longitudinal cracks have been shown to be highly sensitive to changes in pressure in linear-elastic materials (Al-Khomairi 2005; Greyvenstein and van Zyl 2006; Cassa and van Zyl 2011); therefore, the coupled effect of the crack sensitivity and material rheology results in a complex leakage response. The generalized form of Eq. (1) cannot, therefore, accurately capture the true dynamic behavior of such leaks.

Viscoelastic Characterization

Pipe material rheology has an important influence on the behavior of leaks in water distribution system pipes (Ferrante 2012). The pressure-leakage relationship in materials where there is a linear relationship between material stress and strain has been studied in detail (Cassa et al. 2010; De Miranda et al. 2012). However, studies considering the effect of viscoelasticity on this relationship, i.e., the interdependence of stress and strain with time (Benham et al. 1996), are limited. Such studies do, however, present an important initial insight into the influence of the material rheology which results in a nonbijective relationship between pressure and leakage, confirming the inadequacy of leakage exponent modeling approaches (Ferrante 2012; Massari et al. 2012).

Materials, including polyethylene, are classified as viscoelastic due to their composition and structure, which results in a characteristic combination of Hookean elastic behavior and Newtonian viscosity (Wood-Adams et al. 2000). There are three important phases when considering the structural response of viscoelastic materials, namely, creep, relaxation, and recovery. Creep is defined as the time and temperature-dependent strain of a material for a constant stress. Stress relaxation is the time and temperature decrease in stress at a constant applied strain. Recovery is the time and temperature-dependent strain recovery following removal of an applied stress.

In order to model the described viscoelastic characteristics, constitutive equations may be employed to mathematically represent the physical phenomena assuming linear-viscoelastic behavior. Linear viscoelastic constitutive equations are based upon the effects of sequential changes in strain or stress, assuming that all changes are additive (Ferry 1961). Also known as the rheological equation of state, the constitutive equations deal with the time-dependent relationship between stress and strain (Ferry 1961). A formulation of the constitutive equation, shown in Eq. (2) as the convolution integral for strain, defines the time-dependent strain in terms of the loading history (applied stress) and the theoretical material creep compliance, J

$$\epsilon(t) = \int_{-\infty}^{t} J(t-t')\frac{d\sigma}{dt}(t')dt' \tag{2}$$

To implement the theoretical rheological equations of state, a method to calibrate the material response (e.g., creep compliance) is required. The constitutive equations for viscoelasticity may, therefore, be conceptualized as a series of springs, representative of the linear-elastic response, and dashpots, representative of the time-dependent viscous response of a material (Lemaitre et al. 1996). A range of configurations have been developed for application in viscoelastic modeling in biomechanics, fluid mechanics, and polymer science. The generalized Kelvin-Voigt model, shown in Fig. 1, consists of a single Hookean spring and a user-defined number of Kelvin-Voigt elements in series

$$J(t) = J_0 + \sum_{n}^{N} J_n(1 - \exp^{(-t/\tau_n)}) \tag{3}$$

$$\epsilon(t) = \sigma(t)J_0 + \int_{0}^{t} \sigma(t-t')\frac{dJ}{dt'}(t')dt' \tag{4}$$

Eqs. (3) and (4) define the generalized Kelvin-Voigt creep compliance formulation and the time-dependent material strain equation, respectively. The capability of this model in representing the behavior of polymeric materials in hydraulic systems has previously been shown when accounting for the effect of viscoelasticity on pressure transients in water distribution pipes (Bergant et al. 2008; Covas et al. 2004). Some of the key considerations when

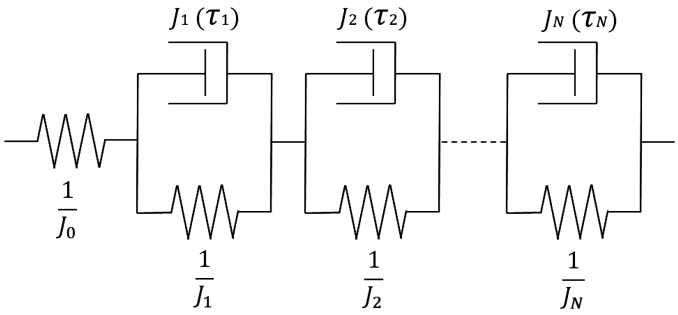

Fig. 1. Schematic of the generalized Kelvin-Voigt model

developing an effective viscoelastic model include the magnitude and scale of the defined or calibrated retardation time periods and model parsimony.

Investigation Aims

The aim of the research reported here was to understand the behavior of longitudinal slits in pressurized viscoelastic pipes, specifically the interaction between the structural dynamics and leak hydraulics, through physical observations. Experiments were conducted to quantitatively assess whether leak area is the primary independent parameter influencing the sensitivity of leakage to pressure, confirming the suitability of the orifice equation in describing such dynamic leaks. Ultimately, the objective of the study was to utilize the developed knowledge and quantitative experimental data to produce an explicit empirically calibrated leakage model for a longitudinal slit in a viscoelastic pipe.

Experimental Setup

A series of experiments were undertaken, which recorded for the first time the synchronous pressure head, leak flow rate, leak area, and material strain under quasi-steady-state conditions (slowly changing) for engineered longitudinal slits in MDPE pipe. Repeatable test conditions were employed to characterize the long-term leakage behavior, specifically the structural response and the associated leak hydraulics under controlled conditions. Simultaneous measurements of the material axial strain and leak area were employed to explore the theory that localized strain is a predictor of the variable leak area.

Laboratory Facility

The laboratory investigation used the contaminant ingress into distribution systems (CID) facility at the University of Sheffield, which is a 141-m-long recirculating pipe loop. The facility consists of 50-mm nominal diameter 12 bar rated MDPE pipe, tensile yield stress of 15 MPa, with water fed from an upstream holding reservoir (volume of 0.95 m^3) through a 3.5-kW Wilo (Burton Upon Trent, U.K.) MVIE variable speed pump. A 0.8-m removable section of pipe, 62 m downstream of the system pump, allows for the inclusion of different test sections housed within a 0.45 m^3 capacity box containing a single side viewing window. The flow rate and pressure data are recorded using a single Arkon (Brno, Czech Republic) Flow System Mag-900 electromagnetic flow meter located immediately downstream from the system pump and a series of Gems (Plainville) 2200 pressure sensors. Data were acquired at 100 Hz using a National Instruments (NI) (Newbury, U.K.) USB-6009 data acquisition device (DAQ) and a Measurement Computing (Newbury, U.K.) PMD1820 DAQ for flow rate and pressure, respectively. Isolation of different sections of the pipe loop is achieved through the use of quarter-turn butterfly valves located at intervals along the pipe, including either side of the test section box. A schematic and image of the facility, relevant to the testing presented in this paper, is shown in Fig. 2.

Test Section Preparation

Manufactured test sections containing longitudinal slits were produced as listed in Table 1, with all sections produced using the same specification pipe as the main pipe loop. The pipe dimensions, 50-mm internal diameter and 6.5-mm wall thickness, classify the pipe as thick-walled because the nondimensional diameter to wall thickness ratio is less than 20 ($d/s = 9.69$). Pipe test sections were cut to 0.8-m length and compression fittings attached to allow for installation within the pipe loop. The use of compression fittings for installation and the resulting induced longitudinal stresses were assumed as having negligible influence on the structural behavior of the leak openings as concluded by Cassa and van Zyl (2011). Three repeat sections were manufactured for testing containing slits 60 mm long and 1 mm wide. A single pass of a 1-mm-thick circular slitting saw was conducted to minimize variation of the initial area negated the influence of the closure effect (compression) of the residual stresses upon removal of the material for each of the three repeat 60 × 1 mm test sections. The slit tips were then rounded using a 1-mm-diameter drill bit to prevent axial propagation of the slits under the applied loading conditions.

Structural Response Measurements

Unique to this study was the simultaneous measurement of leak area and axial strain. Quantification of the leak area was required for assessment of the structural behavior of the leak, and hence the dependence of the leak hydraulics on the time and pressure-dependent response (synchronous leak flow rate and associated discharge coefficient). A range of potential methods for measuring the leak area were assessed including Moire interferometry (Yen and Ratnam 2010) and laser scanning (Rabah et al. 2013); however, an image analysis technique was concluded to be the most effective and nonintrusive method providing high accuracy, efficiency, and simplicity. To accurately distinguish between the outside of

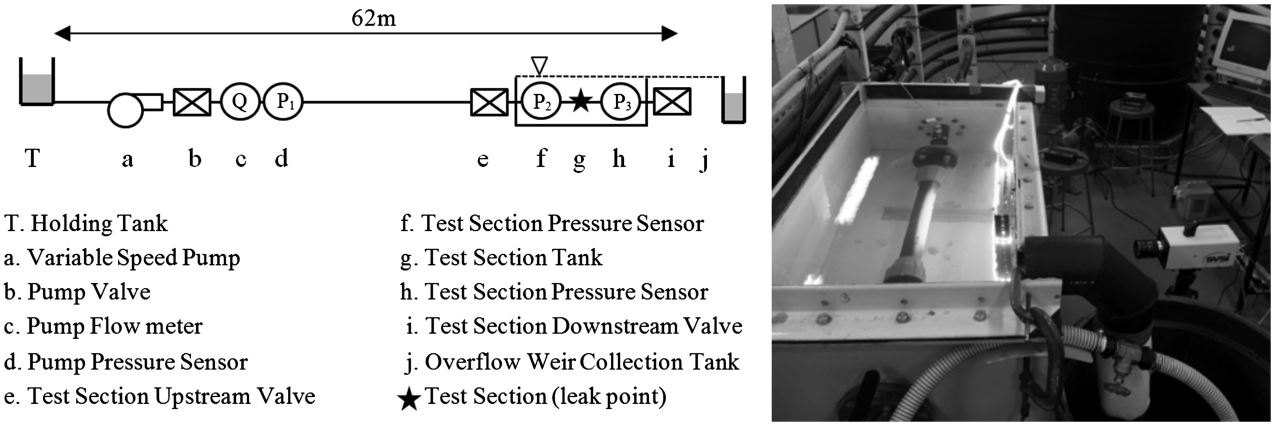

Fig. 2. Contaminant ingress into distribution systems laboratory schematic and image of the test setup

Table 1. Summary Table of Test Sections and Details of Axial Strain Gauge Locations

Name	Length/ width (mm)	Initial area (m^2)	Test pressure heads (m)	SG location (r, θ, z)
TS601a	60/1	3.78×10^{-05}	10, 20, 25	31.5, 0.588, 0
TS601b	60/1	4.25×10^{-05}	20	31.5, 0.531, 0
TS601c	60/1	4.63×10^{-05}	20	31.5, 0.543, 3.0

Note: Strain gauge (SG) locations are listed as cylindrical coordinates (r, θ, z), where r = radial coordinate (mm); θ = azimuthal coordinate (rad); and z = axial coordinate (mm).

the pipe and the leak opening, the pipe surface was painted white using an enamel spray paint. This provided a clear distinction between the white surface of the pipe and the black area of the slit opening. Images of the test section were recorded using a GigaView (Huntsville, Alabama) SVSI high-speed camera at 3 frames per second (fps), allowing for continuous image capture over a maximum 8-h time period. The section was illuminated by an array of IP65 (ANSI/IEC 2004) rated bright white strip light-emitting diode (LED) lights, which provided a consistent light source with minimal heating effect. A basic image-processing methodology was then employed to convert the red/green/blue (RGB) images to binary form using a defined constant threshold value as shown by way of example in Fig. 3. A pixel count of the black pixels, i.e., slit opening, was then completed to calculate the leak area with a maximum associated error of approximately ± 3.82 mm^2 related to the image resolution and the coupled effect of the lighting and threshold value. A calibration image was used to quantify the physical area of each pixel prior to testing.

It has previously been surmised that material strain can be used as an indicator of the dynamic area of leaks in pressurized pipes (Ferrante 2012). In order to determine the relationship between the synchronous material strain and leak area and whether the strain may be used, a predictor of dynamic leak area, a selection of TML GFLA-3-50 (Tokyo, Japan) strain gauges were attached using CN (Tokyo, Japan) cyanoacrylate adhesive to the pipe in the axial pipe direction in discrete locations as listed in Table 1. Only axial strain measurements parallel to the slit length were selected for the experimental work because theoretically they presented the greatest potential relationship between localized material strain and leak area based on the mode of deformation, i.e., tensile strain along the length of the slit wall. This was confirmed in a preliminary phase of testing. A cylindrical coordinate system (r, θ, z) is used to describe the location of the gauges [approximate coordinate error $\pm(0$ mm, 0.0048 rad, 1.5 mm)] as shown in Fig. 4, where (31.5, 0, 0) is the center of the slit area at the external radius of the pipe. Strain data were acquired at 100 Hz using NI 9944 quarter-bridge completion accessories connected by RJ50 leads (National Instruments, Newbury, U.K.) to a NI 9237 four-channel module housed within a NI CompactDAQ chassis. The strain gauges were waterproofed using flexible rubber mastic tape applied over the surface of the gauge, which was shown to have negligible effect on both the structural behavior of the leak and the measurements recorded by the strain gauges.

Experimental Procedure

The experimental procedure aimed to effectively record the relationship between the structural and hydraulic behavior of a leak through the simultaneous measurement of four key parameters (pressure head, leak flow rate, leak area, and axial strain). The conservative but controlled system conditions were defined to produce data capturing the time-dependent viscoelastic behavior (creep and recovery characteristics) coupled with the leakage response. The procedure comprised two cyclic stages: (1) pressurization and resulting creep phase, and (2) depressurization and resulting recovery phase. Stage 1 provided data on the time-dependent leak behavior following the assumed instantaneous pressurization and ensuing quasi-steady-state conditions at a predefined initial pressure head, with Stage 2 providing data on the leak opening area behavior following the assumed instantaneous depressurization and material recovery. Three to five repeats were conducted for TS601a at predetermined initial pressures of 10, 20, and 25 m head, each of which included an 8-h pressurization phase and 16-h recovery phase. Fig. 5 summarizes the experimental procedure implemented for the pressurization and recovery phases. The lengths of time for the pressurization and depressurization stages were chosen due to the observed time periods of measurable

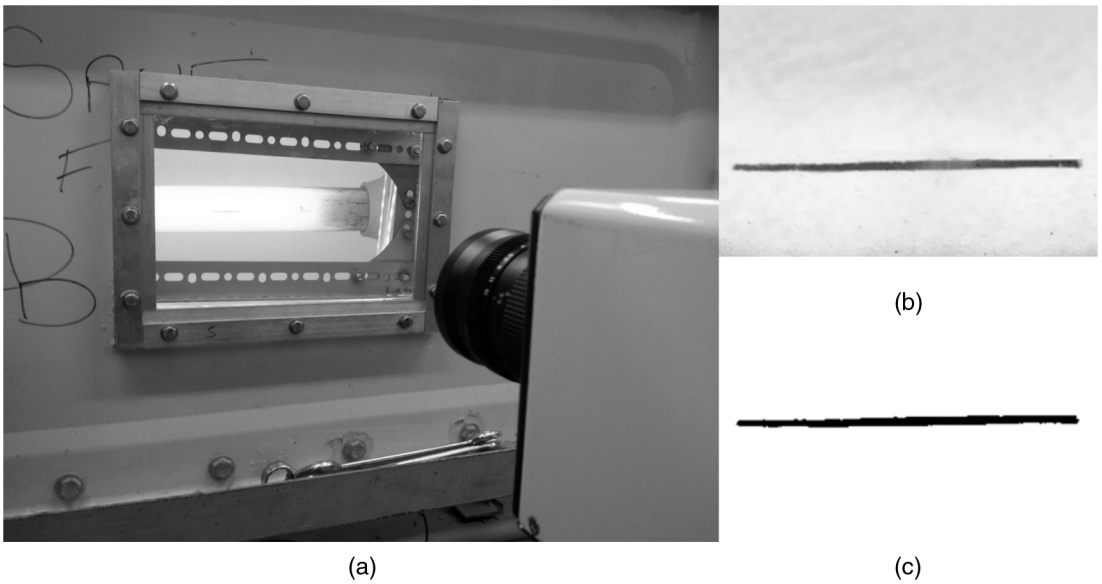

Fig. 3. (a) Camera setup for image capture (3 fps) of horizontally orientated 60×1 mm longitudinal slit; (b) raw image; (c) processed binary image of slit

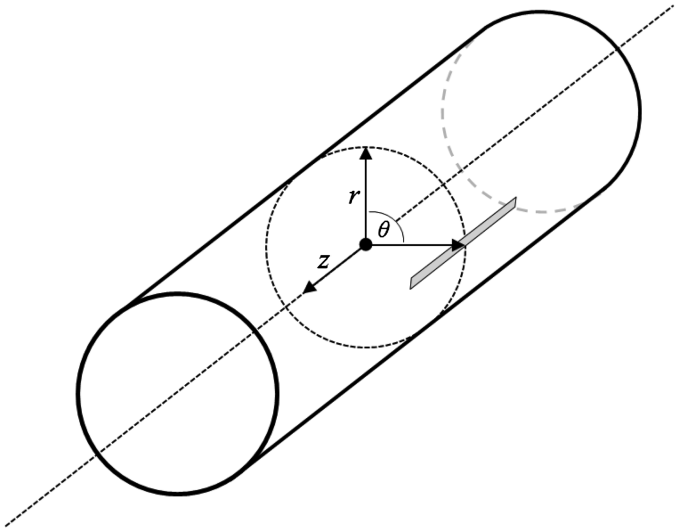

Fig. 4. Cylindrical coordinate system for strain gauge location (Table 1) where the center of the leak area is located at (31.5, 0, 0)

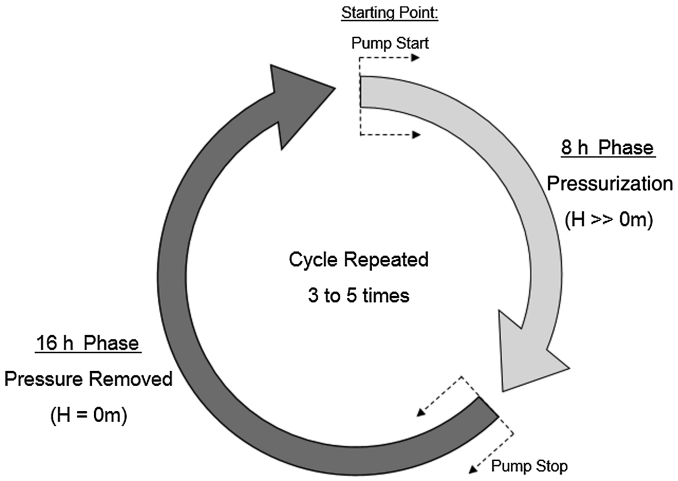

Fig. 5. Experimental procedure flowchart, defining the pressurization (8-h phase) and recovery (16-h phase) stages used to capture the creep and recovery responses, respectively

structural creep and recovery during preliminary testing. The repeated test sections, TS601b and TS601c, were both tested at 20-m initial pressure head only, primarily for assessment of experimental repeatability. The pressures utilized within the experimental work represent relatively low pressures compared with operational water distribution system pressures, but were set due the physical constraints (e.g., size of overflow weir) of the laboratory facility.

After the installation of the individual test sections within the pipe loop, the system was left dormant for 2 days to allow equilibration of the material strain. A null offset for all the attached strain gauges was executed prior to testing, assuming the test sections were at rest (zero stress and strain). The pressurization phase was conducted by starting the pump at a predetermined speed to achieve the necessary initial system pressure head. A manual opening of the upstream test section box valve (item *e*) while the downstream test section box valve remained closed was completed resulting in a step pressure change in the test sections. The subsequent leakage flow rate was allowed to overflow the box into the collection tank before being returned to the main system holding tank by a separate automated submersible pump, thus maintaining a constant water level within the test section tank ($H_w = 0.45$ m). After the defined 8-h creep period, the upstream valve was closed, resulting in a step change depressurization and isolation of the test section. The test sections were then left to complete the 16-h recovery phase before repeating the process. Tests were conducted between 3 and 5 days to allow for a detailed assessment of the effect of the loading time history on the material response.

Experimental Results

The leakage behavior of the longitudinal slits in MDPE pipe were characterized using four synchronous measurements of leak area, material strain, pressure head, and subsequent leakage flow rate. The results for the three test sections investigated (as described in Table 1) are presented in Figs. 6–8, showing the 5-day response to a series of equal 20-m pressure head pressurizations and depressurizations for TS601a and the equivalent 3-day responses for TS601b and TS601c. Each figure shows the measured leak area (hollow black circles) and associated axial strain (solid grey line), along with the recorded pressure head (gray dots), measured at item *h* in Fig. 2, and the system flow rate (black squares), which is equal to the leakage flow rate.

The observed leak area behavior comprised an instantaneous elastic response following loading and unloading, with subsequent time-dependent viscoelastic creep and recovery phases. There is a discernible difference in the structural response of the leak opening on the first loading phase compared with the subsequent loading phases, encapsulated by the relative curvature (shape) of the leak area and axial strain data. The large scatter in the measured area of TS601b and TS601c compared with TS601a was due to distortion of the discharging jet and resulting interference of the slit imaging process. This directly affected the clarity and accuracy of the area measurement during the pressurization phases only, although the lower bound of the scattered area data for TS601b is believed to be a good representation of the actual leak area. The higher recorded flow rates for TS601b and TS601c relative to TS601a and the specific slit face roughness are surmised to be the primary causes of this jet distortion. While quantification of the actual leak area is not feasible due to the large scattering in the pressurized area data, this does not compromise the whole data set, notably the recovery leak area. The equivalence in the observed characteristic shape of the simultaneous strain and leak area measurements (recovery phase data for TS601b and TS601c only) confirms qualitatively that the axial strain may be used as a predictor of the leak area. The pressure data show an approximate linear decrease during the discrete pressurization phases, with a maximum difference of −1.0 m recorded for a single repeat test over the 8-h time period. This head loss is coupled with the nonlinear increase in leak flow rate over the same time period associated with the predefined constant pump speed. Observed increasing step changes in the measured leak flow rate were associated with the expulsion of partial blockages from the leak opening due to residual debris in the system flow. Such changes are coupled with step decreases in both pressure head and axial strain, although the magnitude of the expected change of area is surmised to be less than the resolution of the area measurement technique.

A daily temperature increase was noted and an increase across the full times series data set, with a minimum temperature of 18°C and a maximum temperature of 24°C recorded. However, the average temperature increase during each discrete pressurization phase

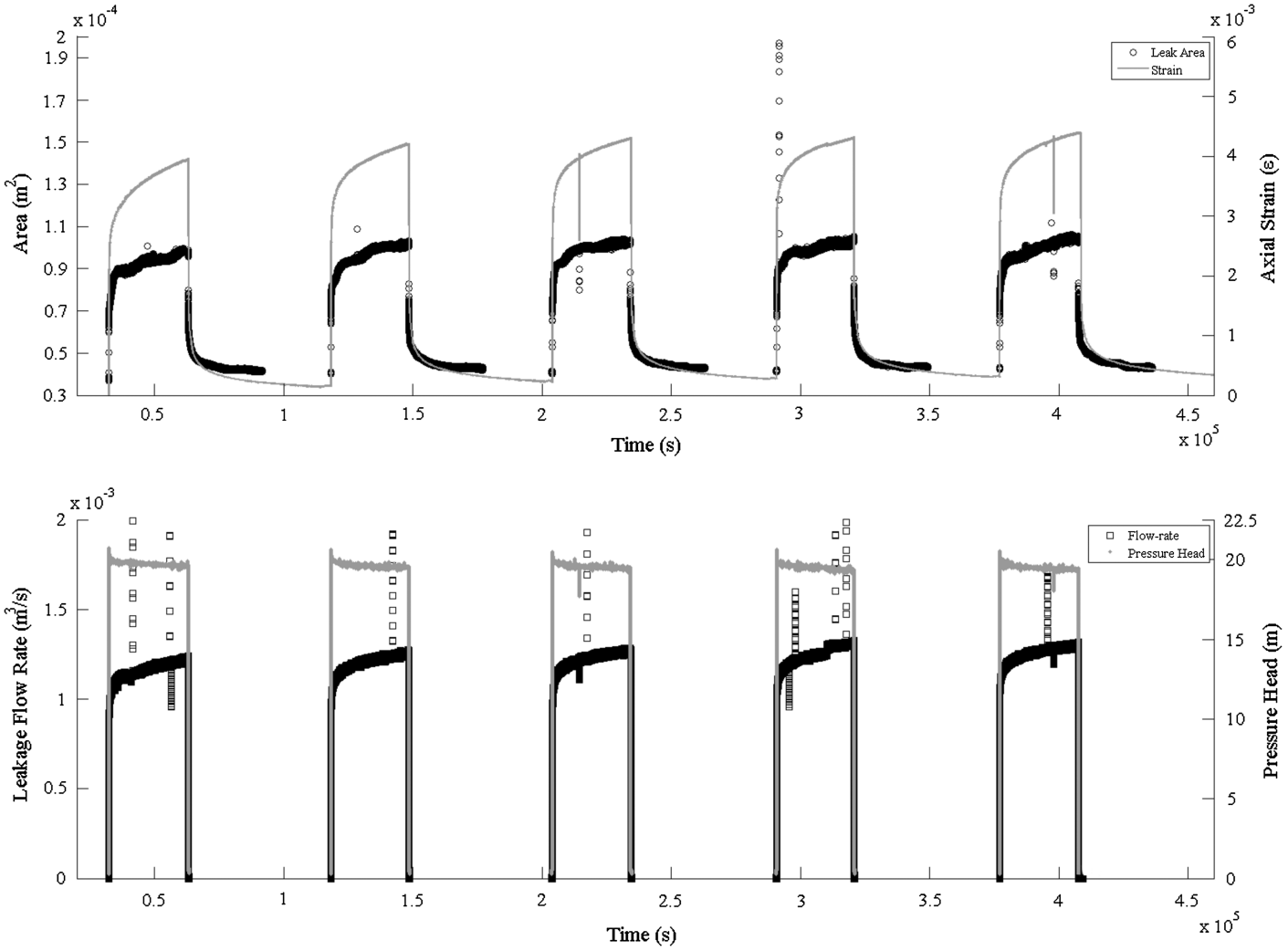

Fig. 6. Compiled 5-day measurements of leak area, axial strain, leak flow rate, and pressure head for TS601a at 20-m initial pressure head

was approximately 3°C. The heating effect of the system pump is surmised as being the primary cause of the noted temperature rise based on preliminary testing. The daily temperature rise had negligible influence on the strain gauge measurements and is assumed to have had an insignificant influence on the characterized viscoelastic response.

The results presented in Figs. 6–8 highlight the repeatability of the characteristic behavior of the three 60×1 mm longitudinal slits subject to the same system conditions. Equivalent results for TS601a at 10- and 25-m pressure heads are not presented in detail herein, but correspond closely with the observed characteristics highlighted for the three repeated test sections of all four of the key experimental parameters.

Analysis

To substantiate the use of strain as a predictor of the leak area, the relationship between these two parameters was quantified. Fig. 9 is a plot of the measured axial strain for all three test sections against the concurrent measured leak area. Area data from the depressurization phases only were utilized for the calibration of TS601b and TS601c due to the interference in the image leak area definition as previously described. The mean relationships between the measured axial strain and leak area may be represented by simple linear equations for each test section, as listed in Table 2.

The use of recovery phase (depressurization) data only for the fitting procedure for TS601b and TS601c results in relatively low root-mean-square error (RMSE) due to the lower range of area and axial strain magnitude. The equations describing the association between strain and area allow for further analysis of the interaction of the structural behavior and leak hydraulics where there is uncertainty with regards to the leak area during pressurization.

Leak Hydraulics

Fig. 10 shows the evaluated discharge coefficients using the orifice equation ($\lambda = 0.5$) and the recorded laboratory data (synchronous leak flow rate, leak area, and pressure) for the three test sections. The raw data were filtered to reduce the total number of data points resulting in a representative data sample equivalent to a sampling rate of 1 Hz. The mean discharge coefficient values were 0.642 [standard deviation $(\sigma) = 0.036$], 0.5443 ($\sigma = 0.078$), and 0.488 ($\sigma = 0.079$) for TS601a, TS601b, and TS601c, respectively, at 20-m pressure head. The corresponding mean discharge for coefficient values for TS601a at 10- and 25-m pressure heads were 0.608 ($\sigma = 0.0062$) and 0.642 ($\sigma = 0.0085$), respectively. The distinctly reduced C_d value for TS601c may be accounted for by the measured leak area error previously noted. The results presented in Fig. 10 confirm that for individual longitudinal slits in pressurized pipe, a constant discharge coefficient is applicable to describe the

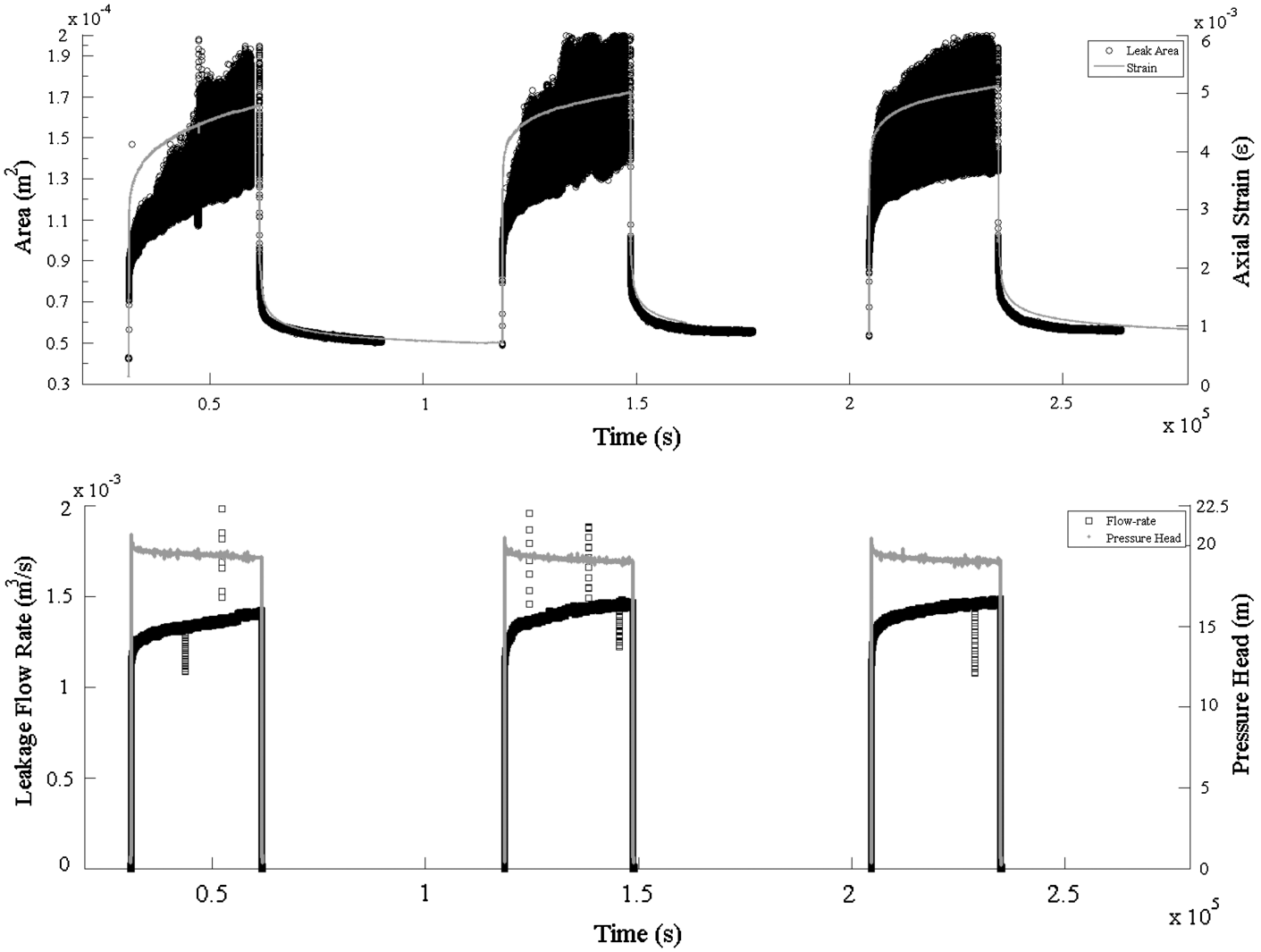

Fig. 7. Compiled 3-day measurements of leak area, axial strain, leak flow rate, and pressure head for TS601b at 20-m initial pressure head; plotted on the same axis as Fig. 6 to aid comparison

pressure and time-dependent discharge through the leak. This supports the appropriateness in the application of orifice theory within leakage modeling of dynamic leaks provided that the synchronous leak area can be accurately estimated.

Structural Response and Leakage Model

The direct relationship between axial strain and leak area provides a means to predict the time-dependent leak area for individual test sections if the localized material strain could be known or modeled. The definition of a viscoelastic model for the pressure and time-dependent axial strain may, therefore, be useful as a predictor of the actual leak area and hence leakage flow rate. A rigorous calibration using the experimental data from TS601a was conducted in order to define a model for the dynamic axial strain and hence the dynamic leak area. The generalized Kelvin-Voigt mathematical representation of viscoelastic behavior was chosen for the calibration due to its efficiency and previous effective use in modeling viscoelastic pipes under transient loading conditions. A nonlinear least-squares methodology was employed using the Levenberg-Marquardt algorithm and a function tolerance of 1×10^{-12} to fit the creep compliance terms (J_n) as given in Eq. (3), using the measured strain, pressure head data, and the convolution integral, Eq. (4). Calibration of the discrete daily leakage response and the 5-day response were evaluated. The results of the calibration program considering the full time history (5-day response) are summarized in Table 3. The retardation times (τ_n) were assigned prior to the calibration to capture the discrete time period material response. These predetermined values were used to represent the time periods in increasing orders of magnitude (multiples of 10 s) covered by the long-term response of the structural behavior captured within the experimental program. This methodology reflected the method used by Covas et al. (2005) when considering the calibration of the short-term viscoelastic response of pipes to transient propagation.

Employing the 11-component parameter model as detailed in Table 3, the strain data were converted to time-dependent modeled leak area [$A_L(t)$] using the calibration for TS601a given previously. The 11-component model was assessed to be the optimal model selection based on computational efficiency and modeling accuracy (standard error representative of approximately 11.3% of the experimental recorded standard deviation). The mean value for the evaluated discharge coefficient ($C_d = 0.64$) based on the analysis presented in Fig. 10, the measured differential pressure head across the leak opening, and the modeled leak area were input into Eq. (5), a modified time-dependent form of the orifice equation, to evaluate

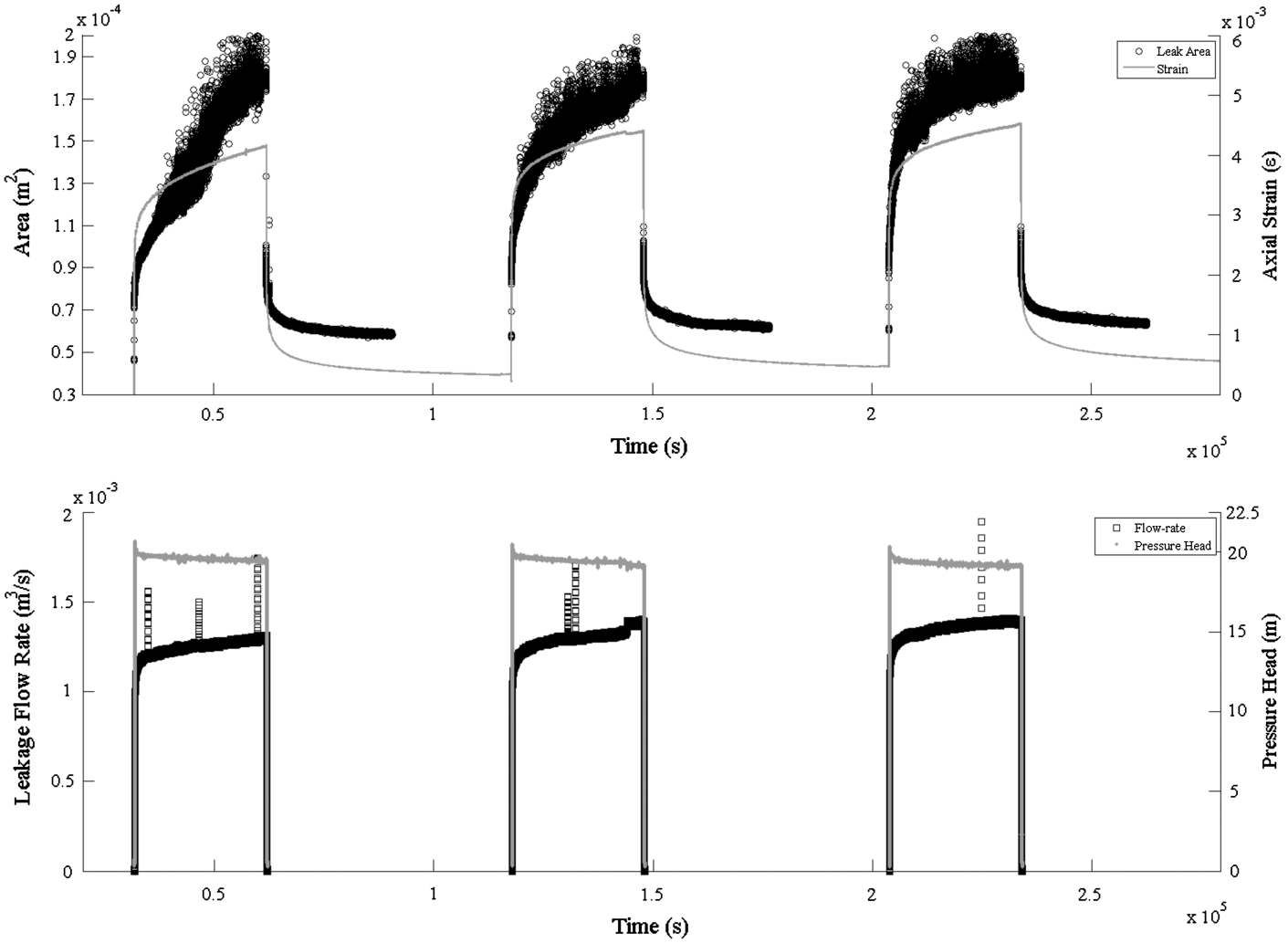

Fig. 8. Compiled 3-day measurements of leak area, axial strain, leak flow rate, and pressure head for TS601c at 20-m initial pressure head; plotted on the same axis as Fig. 6 to aid comparison

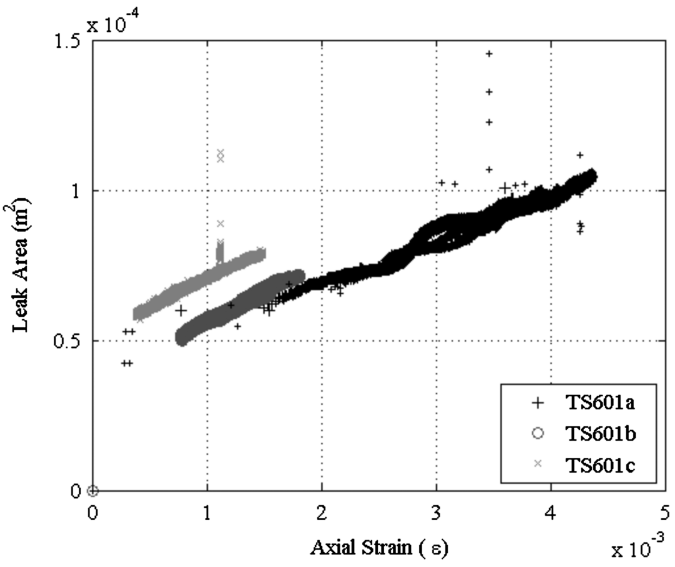

Fig. 9. Leak area and strain relationship as measured for TS601a, TS601b, and TS601c; measurements of leak area and axial strain during the recovery phase only are presented for TS601b and TS601c

Table 2. Linear Fitting Parameters for the Explicit Strain Area Relationship for Three Discrete Test Sections

Test section	Gradient	Intercept (m^2)	RMSE (m^2)
TS601a	0.0176	2.8×10^{-5}	2.25
TS601b	0.0199	3.6×10^{-5}	0.57
TS601c	0.0197	5.1×10^{-5}	0.50

the leakage through the longitudinal slit. Eq. (6) is the leak area model using the calibrated creep compliance model (where J_{11} is the 11-component creep compliance model [Eq. (3)] using components listed in Table 3) and the linear strain area relationship for TS601a where $C_1 = 0.01765$ and $C_2 = 2.8 \times 10^{-5}$. Fig. 11 presents results from this procedure for TS601a at three discrete quasi-steady-state pressure heads (10, 20, and 25 m) alongside the measured leak flow rate from the experimental work showing extrapolation across pressure ranges is valid

$$Q(t) = A_L(t) C_d \sqrt{2gH(t)} \tag{5}$$

$$A_L(t) = C_1 \left[\rho g \int_0^t H(t-t') \frac{dJ_{11}}{dt'}(t') dt' \right] + C_2 \tag{6}$$

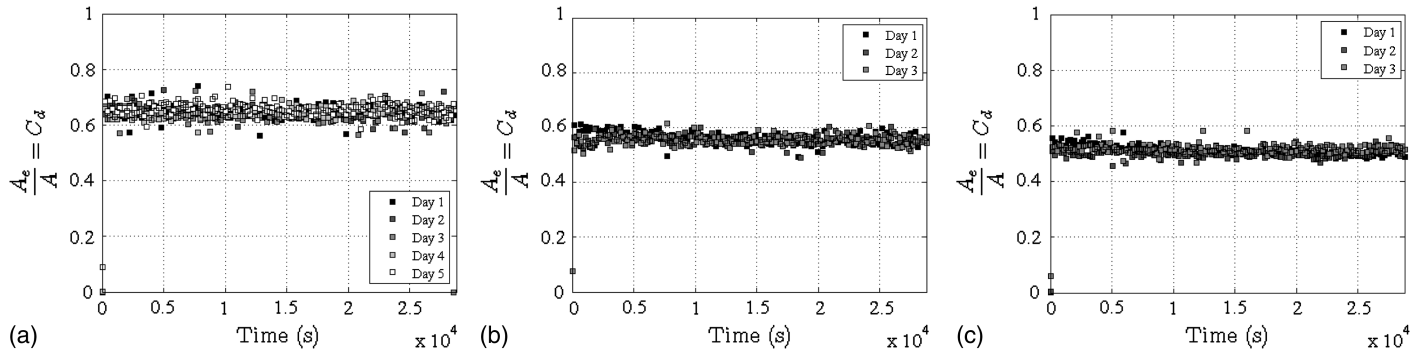

Fig. 10. Calculated discharge coefficients for (a) TS601a; (b) TS601b; and (c) TS601c at 20-m pressure head

Table 3. Nonlinear Least-Squares Calibration of Creep Compliance Components for Time-Dependent Axial Strain for TS601a

J_n(1/Pa):		J_1	J_2	J_3	J_4	J_5	J_6	J_7	Standard
τ_n (s):	J_0	10	100	1,000	10,000	100,000	1,000,000	10,000,000	error
Three components	8.5×10^{-09}	1.26×10^{-08}	0	0	0	0	0	0	5.16×10^{-04}
Five components	8.5×10^{-09}	1.00×10^{-11}	1.26×10^{-08}	0	0	0	0	0	5.08×10^{-04}
Seven components	8.5×10^{-09}	1.28×10^{-09}	1.00×10^{-11}	1.17×10^{-08}	0	0	0	0	4.53×10^{-04}
Nine components	8.5×10^{-9}	2.00×10^{-09}	5.46×10^{-09}	1.22×10^{-11}	7.46×10^{-09}	0	0	0	2.90×10^{-04}
11 components	8.5×10^{-09}	2.14×10^{-09}	2.84×10^{-09}	4.09×10^{-09}	1.84×10^{-09}	8.42×10^{-09}	0	0	1.92×10^{-04}
13 components	8.5×10^{-09}	2.04×10^{-09}	3.02×10^{-09}	3.89×10^{-09}	2.15×10^{-09}	6.68×10^{-09}	6.13×10^{-09}	0	8.31×10^{-05}
15 components	8.5×10^{-09}	2.81×10^{-09}	2.85×10^{-09}	2.99×10^{-09}	2.66×10^{-09}	5.93×10^{-09}	7.80×10^{-09}	1.26×10^{-11}	8.49×10^{-05}

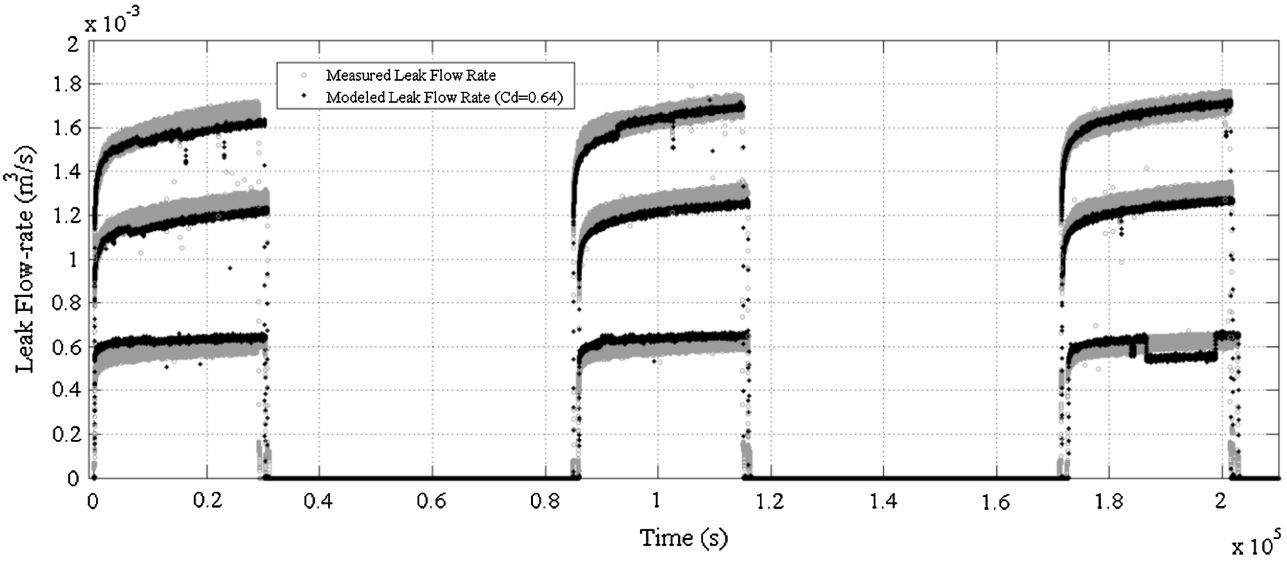

Fig. 11. Comparison of measured and modeled leakage from TS601a for 3-day pressure tests (downsampled to 1 Hz); quasi-steady-state pressure heads of 10, 20, and 25 m in ascending order in plot

Comparison of the net 3-day leakage volumes produced percentage errors of −4.29, 3.22, and 0.14% between the modeled and measured leakage volumes for the 10-, 20-, and 25-m pressure head tests, respectively, further confirming the validity of the developed explicit model.

Discussion

The research presented herein aimed to physically quantify the dynamic leakage behavior of longitudinal slits in viscoelastic pipe, characterizing the structural dynamics and the associated leakage hydraulics. Three test sections containing artificially manufactured longitudinal slits were produced for the experimental investigation by removing material from the pipe. The noted difference in the initial areas of the three 60×1 mm sections presented was due to the precision of the cutting process and influence of the localized material residual stress distribution as well as the accuracy of the leak area measurements. However, the characteristic leakage behavior was consistent for all three test sections, with the relative variance in leak flow rate a function of the initial leak area. In reality, longitudinal cracks do not typically result from the removal of

material but may occur due to chemical degradation of the material (Duvall and Edwards 2011), slow crack growth (Brown 2007), or fatigue (Nishimura et al. 1993), and would therefore have an imperceptible opening area at zero pressure. It is not anticipated that the associated characteristic behavior would vary significantly from the observations made herein for cracks with zero area at rest, although the localized crack tip stresses would be higher, resulting in an increased risk of crack propagation and structural failure of the pipe.

Leak Area versus Localized Material Strain

Analysis was conducted to evaluate the average maximum change of area for all the test sections during the first 8 h of the recovery phases: -6.38×10^{-05} m^2 ($\sigma = 2.76 \times 10^{-06}$ m^2), -6.10×10^{-05} m^2 ($\sigma = 1.50 \times 10^{-06}$ m^2), and -5.99×10^{-05} m^2 ($\sigma = 1.79 \times 10^{-06}$ m^2) for Days 1, 2, and 3, respectively. The low standard deviations for the repeated test sections suggest that the susceptibility and magnitude of longitudinal slits to deformation is dependent primarily on the slit length not the width, which varied across the length of each manufactured slit resulting in different initial areas. This corresponds to the findings from numerical simulations conducted by Cassa and van Zyl (2011) investigating the structural behavior of equivalent leaks in linear-elastic materials. The discrepancy in the relative magnitude of strain for each test section corresponds to the distance of the strain gauge from the slit edge. In other words, the material strain is a function of the proximity to the slit. Further analysis of the axial strain distribution parallel and perpendicular to the leak length through physical observations and numerical simulations would advance the understanding of the mechanism of opening, i.e., whether deformations are due to localized buckling or bulging of the material. An evaluation of the significance of the manufacturing process on the inherent stresses within the extruded pipe may also provide a greater level of understanding of the observed phenomena.

The validated relationship between the measured leak area and the localized material axial strain allows for evaluation of the synchronous dynamic leak area if the strain is known or can be modeled. The simple fitted linear equations provide an alternative means to define the time-dependent leak area if the leak is not visible, i.e., buried. The influence of the external ground conditions on the leakage behavior of dynamic leaks (e.g., transferred loading, soil hydraulics, additional flow resistance, and ground temperature) remains a comparatively unexplored area of research. This unique data set and the calibration between leak area and strain, therefore, provides an opportunity to develop a methodology to explore the performance of buried leaking pipes, assessing the fluid-structure interaction and the associated structural dynamics and leak hydraulics, addressing the limited current knowledge on this topic.

The temperature range recorded during testing means that the magnitude of the observed structural deformations may be considered as relatively more extreme than for pipes in situ due to the relationship between temperature and creep compliance, i.e., increasing temperature reduces the stiffness of the material. The typical seasonal soil temperature variations in the United Kingdom for pipe burial depths between 750 and 1,350 mm (Water Regulation No. 1148 1999) lie between 4 and 21°C (Banks 2012).

Discharge Coefficient

It is generally agreed that the dynamic leak area is the dominant influence on the observed sensitivity of leaks to pressure (Clayton and van Zyl 2007; Cassa and van Zyl 2011; Ferrante 2012). This interpretation is qualitatively supported by the discernible linear correlation between the measured leak area and flow rate from the experimental results. Studies have previously used an effective leak area when modeling leakage due to the uncertainty of the changing leak area and the potential dependence of the associated leak discharge coefficient. Using the synchronous measurements of the leak flow rate, pressure head, and leak area, the time-dependent discharge coefficients for each test section were evaluated and found to remain constant over the full range of testing (five discrete loading phases) despite a maximum change in leak area of greater than 250% for TS601a at 20-m pressure head, for example. Two additional test sections with longitudinal slits of 20×1 and 40×1 mm were subsequently produced to confirm this finding, with calculated mean discharge coefficients of 0.608 ($\sigma = 0.0091$) and 0.610 ($\sigma = 0.0062$), respectively. It may, therefore, be assumed that the theoretical discharge coefficient is independent of the leak deformation but dependent on the orifice type. This provides confirmation that the structural behavior, namely, the change of leak area, is the most critical determining factor of the dynamic leakage behavior. Ultimately this validates the inference made that accurate leakage models based on the orifice equation may be utilized for longitudinal slits in thick-walled viscoelastic pipes under fully turbulent flow conditions. This is achievable by using a discrete constant discharge coefficient, knowledge of the applied time-series pressure, and the synchronous leak area quantified from physical data or structural modeling. In reality, the actual leak area may not be measurable. However, knowledge that the discharge coefficient is independent from the dynamic structural leak behavior may, therefore, allow an approximation of the leak type and area to be made based on the observed pressure and leakage relationship. Further work to confirm this observation (constant discharge coefficient) for other leak types in different pipe materials is still required but remains a commonly adopted assumption (e.g., Cassa et al. 2010).

Viscoelasticity Modeling

A generalized Kelvin-Voigt creep compliance formulation [Eq. (4)] was employed within the viscoelastic calibration due to the effectiveness of this mathematical representation in capturing both the instantaneous elastic and time-dependent creep and recovery material responses over specified time periods. As may be expected, the results of the calibration show that the greater the number of creep compliance components the better the fit to the experimental data, highlighting the importance of employing both the short- and long-term components to define a model that considers the full loading-history and the time-dependent creep and recovery responses. Smaller separate models (<11 total components) are capable of accurately predicting the daily strain response in isolation without considering the full loading history. Application of an 11-component model was determined to be the minimum requirement to effectively replicate the observed structural behavior because five discrete retardation time periods were identified from the time-dependent structural response. This, therefore, represents an accurate and parsimonious model essential in the development of computationally efficient tools for use within both academic and industrial applications. Separation of the daily standard errors indicated that the calibration goodness of fit was weakest for the first day. This highlights a potential limitation of mathematical representations in accurately predicting the total physical response of viscoelastic structures to applied loading, emphasizing that such models are only ever approximations of the true behavior. This modeling error is inconsequential with regards to the modeling error for application in real systems because it is not anticipated that in reality a leak would either exist in newly laid pipeline that is pressurized for the first time or be present in a pipe that has been

fully depressurized for a time greater than the total material recovery time. The investigation highlights the need to consider the entire loading history, or alternatively a time period greater than the time required for the material to reach a quasi-steady state. Fig. 11 confirms the effectiveness of Eq. (5), a time and pressure-dependent form of the orifice equation, as a means of modeling the leakage behavior of discrete longitudinal slits in MDPE pipe considering the loading history and the interdependence of the structural behavior and the leak hydraulics.

Leakage Modeling

Leakage exponent-based analyses are often used as a means to assess the sensitivity of leaks to pressure. The results presented in this paper question the validity of such an approach when considering viscoelastic materials that not only display pressure-dependence but also time-dependence. The impact of this is in reducing the effectiveness and benefits of leakage assessment and control techniques using the FAVAD (or similar) leakage model for predominantly viscoelastic material-based systems. In order to understand the benefits of pressure management in reducing the total losses in a system comprised of polyethylene pipe, an appreciation of the complex dynamic nature of the leaks in this material must be considered. The explicit leakage modeling technique developed within this paper allows for accurate calculations of time-dependent leakage based on pressure head data and a leak area model calibrated from recorded axial strain data. A leakage model for longitudinal slits in viscoelastic pipe based on the characterization and calibration within this paper considering all parameters including geometry, material rheology, and loading conditions will provide a means to develop a generalized leakage model considering all the significant influencing parameters. The methodology presented for characterizing the leakage behavior may be developed for assessing the equivalent short-term response of leaks subject to dynamic pressures, e.g., pressure transients due to valve closures, pump shutdown, or changes in demand (Collins et al. 2012). Focus on the short-term response has significance for the assessment of contaminant ingress risk associated with the existence of low or negative pressures in water distribution pipes. Likewise, active leakage control techniques such as leak detection and localization based on inverse transient analysis may be greatly enhanced by the inclusion of the pressure and time-dependent orifice equation.

Conclusion

An experimental investigation was conducted to quantify the leakage behavior of longitudinal slits in MDPE pipe due to changing pressure regime, providing a unique data set measuring the synchronous leak flow rate, pressure, leak area, and material strain. The time and pressure-dependent leak area, due to the viscoelastic behavior of the material, is shown to be the critical factor defining the observed dynamic leakage response of the failure type examined. It was shown that localized axial strain measurements may be used as a predictor of the variable leak area. Therefore, using a mathematical representation of the linear-viscoelastic constitutive equations to characterize the strain, a means to model the dynamic leak area, is provided. Integrating such estimation of the time and pressure-dependent leak geometry into the orifice equation yields an effective means to model the leakage flow rate, in which the coefficient of discharge remains constant. The knowledge gained is relevant to better inform the development of leakage management strategies, including pressure management and other active leakage control technologies, aimed at reducing the real losses from water distribution systems.

References

Al-Khomairi, A. M. (2005). "Use of the steady-state orifice equation in the computation of transient flow through pipe leaks." *Arabian J. Sci. Eng.*, 30(1), 33–45.

ANSI/IEC. (2004). "Degrees of protection provided by enclosures (IP Code)." *ANSI/IEC 60529-2004*.

Ávila Rangel, H., and Gonzalez Barreto, C. (2006). "Determinación de parámetros de fuga para fallas longitudinales, en conexiones domiciliarias y en uniones de tuberías en PVC." 24, 15–22.

Awad, H., Kapelan, Z., and Savić, D. (2008). "Analysis of pressure management economics in water distribution systems." *10th Annual Water Distribution Systems Analysis Conf.*, Water-System, Bari, Italy, 520–531.

Banks, D. (2012). *An introduction to thermogeology: Ground source heating and cooling*, Wiley-Blackwell, Oxford, U.K.

Benham, P. P., Crawford, R. J., and Armstrong, C. G. (1996). *Mechanics of engineering materials*, 2nd Ed., Pearson, NJ.

Bergant, A., Tijsseling, A. S., Vítkovský, J. P., Covas, D. I., Simpson, A. R., and Lambert, M. F. (2008). "Parameters affecting water-hammer wave attenuation, shape and timing. Part 1: Mathematical tools." *J. Hydraul. Res.*, 46(3), 373–381.

Brown, N. (2007). "Intrinsic lifetime of polyethylene pipelines." *Polym. Eng. Sci.*, 47(4), 477–480.

Cassa, A. M., and van Zyl, J. E. (2011). "Predicting the head-area slopes and leakage exponents of cracks in pipes." *Urban water management: Challenges and opportunities, computing and control for the water industry*, Centre for Water Systems, Univ. of Exeter, Exeter, U.K., 485–490.

Cassa, A. M., van Zyl, J. E., and Laubscher, R. F. (2010). "A numerical investigation into the effect of pressure on holes and cracks in water supply pipes." *Urban Water J.*, 7(2), 109–120.

Cheung, P. B., Guilherme, V., Abe, N., and Propato, M. (2010). "Night flow analysis and modeling for leakage estimation in a water distribution system." *Integrating Water Systems: Proc., 10th Int. Conf. on Computing and Control in the Water Industry 2009*, J. Boxall and C. Maksimović, eds., Taylor & Francis Group, London, 509–513.

Clayton, C. R. I., and van Zyl, J. E. (2007). "The effect of pressure on leakage in water distribution systems." *Proc. ICE Water Manage.*, 160(2), 109–114.

Collins, R., Fox, S., Beck, S., Saul, A., and Boxall, J. (2012). "Intrusion and leakage through cracks and slits in plastic (MDPE) pipes." *14th Water Distribution Systems Analysis Conf.*, Engineers Australia, Barton, Australia.

Covas, D., Stoianov, I., Mano, J. F., Ramos, H., Graham, N., and Maksimovic, C. (2004). "The dynamic effect of pipe-wall viscoelasticity in hydraulic transients. Part I: Experimental analysis and creep characterization." *J. Hydraul. Eng.*, 42(5), 516–530.

Covas, D., Stoianov, I., Mano, J. F., Ramos, H., Graham, N., and Maksimovic, C. (2005). "The dynamic effect of pipe-wall viscoelasticity in hydraulic transients. Part II: Model development, calibration and verification." *J. Hydraul. Eng.*, 43(1), 56–70.

De Miranda, S., Molari, L., Scalet, G., and Ubertini, F. (2012). "Simple beam model to estimate leakage in longitudinally cracked pressurized pipes." *J. Struct. Eng.*, 10.1061/(ASCE)ST.1943-541X.0000535, 1065–1074.

Duvall, D. E., and Edwards, D. B. (2011). "Field failure mechanisms in HDPE potable water pipe." *ANTEC, 2011*, Society of Petroleum Engineers, TX.

Farley, M., and Trow, S. (2003). *Losses in water distribution networks: A practitioner's guide to assessment, monitoring and control*, IWA Publishing, London.

Ferrante, M. (2012). "Experimental investigation of the effects of pipe material on the leak head-discharge relationship." *J. Hydraul. Eng.*, 10.1061/(ASCE)HY.1943-7900.0000578, 736–743.

Ferrante, M., Massari, C., Brunone, B., and Meniconi, S. (2011). "Experimental evidence of hysteresis in the head-discharge relationship for a leak in a polyethylene pipe." *J. Hydraul. Eng.*, 10.1061/(ASCE)HY.1943-7900.0000360, 775–780.

Ferrante, M., Meniconi, S., and Brunone, B. (2014). "Local and global leak laws. The relationship between pressure and leakage for a single leak and for a district with leaks." *Water Resour. Manage.*, 28(11), 3761–3782.
Ferry, J. D. (1961). *Viscoelastic properties of polymers*, Wiley, Hoboken, NJ.
GPS-UK. (2014). "GPS PE pipe systems UK." ⟨http://www.gpsuk.com/content/1/126/quality-control.html⟩ (Feb. 2, 2015).
Grann-Meyer, E. (2005). *Polyethylene pipes in applied engineering*, Total Petrochemicals, Solvaer, Norway.
Greyvenstein, B., and van Zyl, J. E. (2006). "An experimental investigation into the pressure leakage relationship of some failed water pipes." *J. Water Supply: Res. Technol. AQUA*, 56(2), 117–124.
Koppel, T., Vassiljev, A., Lukjanov, D., and Annus, I. (2009). "Use of pressure dynamics for calibration of water distribution system and leakage detection." *10th Annual Water Distribution Systems Analysis Conference, 2008*, J. E. vanZyl, A. A. Illemobade, and H. E. Jacobs, eds., ASCE, Reston, VA, 1–12.
Lemaitre, J., Ikegami, K., Rahouadj, R., Cunat, C., and Schapery, R. A. (1996). *Handbook of materials behaviour models*, Vol. I, World Scientific, Amsterdam, Netherlands.
Massari, C., Ferrante, M., Brunone, B., and Meniconi, S. (2012). "Is the leak head-discharge relationship in polyethylene pipes a bijective function?" *J. Hydraul. Res.*, 50(4), 409–417.
May, J. (1994). "Leakage, pressure and control." *BICS Int. Conf. on Leakage Control*.
Nazif, S., Karamouz, M., Tabesh, M., and Moridi, A. (2010). "Pressure management model for urban water distribution networks." *Water Resour. Manage.*, 24(3), 437–458.
Nishimura, H., Nakashiba, A., Nakakura, M., and Sasai, K. (1993). "Fatigue behavior of medium-density polyethylene pipes for gas distribution." *Polym. Eng. Sci.*, 33(14), 895–900.
O'Connor, C. (2011). "Plastics today." ⟨http://www.plasticstoday.com/mpw/articles/the-nature-of-polyethylene-pipe-failure⟩ (Feb. 15, 2014).
Ofwat. (2013). "Industry overview." ⟨http://www.ofwat.gov.uk/regulating/overview/⟩ (Feb. 1, 2015).
Pudar, R. S., and Liggett, J. A. (1992). "Leaks in pipe networks." *J. Hydraul. Eng.*, 10.1061/(ASCE)0733-9429(1992)118:7(1031), 1031–1046.
Rabah, M., Elhattab, A., and Fayad, A. (2013). "Automatic concrete cracks detection and mapping of terrestrial laser scan data." *NRIAG J. Astron. Geophys.*, 2(2), 250–255.
Strategic Management Consultants. (2012). "Review of the calculation of sustainable economic level of leakage and its integration with water resource management planning." *EA 26777*, Environment Agency.
Thornton, J., and Lambert, A. (2005). "Progress in practical prediction of pressure: Leakage, pressure: Burst frequency and pressure: Consumption relationships." *IWA Special Conf.—Leakage 2005*, 1–10.
Vitkovsky, J. P., Simpson, A. R., and Lambert, M. F. (2000). "Leak detection and calibration using transients and genetic algorithms." *J. Water Resour. Plann. Manage.*, 10.1061/(ASCE)0733-9496(2000)126:4(262), 262–265.
WaterRegulation No. 1148. (1999). "1999 No. 1148 water industry, England and Wales the water supply (water fittings) regulations 1999." London.
Wood-Adams, P. M., Dealy, J. M., Willem deGroot, A., and Redwine, O. (2000). "Effect of molecular structure on the linear viscoelastic behavior of polyethylene." *Macromolecules*, 33(20), 7489–7499.
Yen, K. S., and Ratnam, M. M. (2010). "2-D crack growth measurement using circular grating moiré fringes and pattern matching." *Struct. Control Health Monit.*, 18(4), 404–415.